ELSEVIER

Journal of Hydrology 254 (2001) 174–198

Journal of Hydrology

www.elsevier.com/locate/jhydrol

Process controls of water balance variability in a large semi-arid catchment: downward approach to hydrological model development

C. Jothityangkoon, M. Sivapalan*, D.L. Farmer

Centre for Water Research, Department of Environmental Engineering, University of Western Australia, 35 Stirling Highway, Crawley, WA 6009, Australia

Received 16 August 2000; revised 9 May 2001; accepted 16 July 2001

Abstract

The process controls on water balance are examined at the annual, monthly and daily scales. A systematic 'downward' approach for the formulation of models of appropriate complexity is presented based on an investigation of the climate, soil and vegetation controls on water balance. Starting with a simple model, complexity is added in steps, with the models tested progressively against signatures of runoff variability at each time scale. The inter-annual variability of runoff is the first signature considered, followed by the intra-annual (mean monthly) variation of runoff. The flow duration curve is the third key signature and is used to test predictions of the daily water balance model. These analyses are carried out using observed data from the Collie River Basin in Western Australia. At the annual time scale, a simple water balance model including saturation excess overland flow and evaporation is found adequate, provided spatial variability of soil depths and rainfall are introduced through multiple buckets. At the monthly time scale, additional processes are required—the key process is subsurface runoff, but in our case we also separated total evapotranspiration into bare soil evaporation and transpiration to represent the heterogeneous vegetation cover. At the daily time scale, inclusion of non-linearity in the storage–discharge relationship for subsurface runoff generation was important, and more crucially, the inclusion of a deeper groundwater store to capture prolonged low flows was important. Model predictions were very sensitive to the assumed distribution of soil depths, both within each subcatchment, and between subcatchments on a regional basis. Streamflow routing was important for large catchments to capture high flows. The overall conclusion is that in this semi-arid catchment, spatial variability of soil depths appear to be the most important control on runoff variability at all time and space scales, followed by the spatial variability of climate and vegetation cover.

Keywords: Process controls; Water balance; Spatial variability; Distributed storage; Downward approach; Water yields

1. Introduction

This paper presents a systematic approach to the development of a long-term water balance model for a large catchment in semi-arid Western Australia. The approach presented is a top-down or downward approach (Klemes, 1983). It involves starting with the simplest model configuration at a large time scale (i.e. annual), and gradually increasing the complexity of the model with decreasing time scales (annual to monthly and finally to daily), in response to an evaluation of the model's predictions against

* Corresponding author. Tel.: +61-9380-2320; fax: +61-9380-1015.

E-mail address: sivapala@cwr.uwa.edu.au (M. Sivapalan).

0022-1694/01/$ - see front matter
PII: S0022-1694(01)00496-6

appropriate 'signature plots' at each time scale. At any stage in this progression, the model configuration must only be as complex as needed to capture the appropriate signature of runoff variability (and no more). The end result is a daily water balance model with parameters estimated mostly a priori, and with minimal calibration. But along the way, the model development will also be used to obtain an appreciation of the process controls of water balance in large heterogeneous catchments in semi-arid climates.

Understanding the heterogeneity of catchment responses resulting from the spatial and/or temporal variability of climate, topography, soils and vegetation is a challenging issue facing hydrology, particularly in respect of the unsolved problem of prediction of runoff from ungauged basins (Gupta and Waymire, 1998). The study of water balance is becoming a major issue since it impacts on the water yield of catchments, especially under the impacts of significant human-induced land use changes. Furthermore, it is increasingly becoming clear that predictions of flood and drought impacts, and of water quantity and quality, cannot be made without a deep understanding of the climatic, vegetation, soil and topographic controls on water balance.

Amongst the current generation of hydrological models we can distinguish two categories, which can be classified as physically-based and conceptual models. Freeze (1978) introduced the first generation of distributed, physically-based models founded on rigorous numerical solution of partial differential equations governing flow through porous media, overland flow and channel flow. These equations also form the basis of other distributed models such as the Systeme Hydrologique Europeen (SHE) model described by Abbott et al. (1986). Lumped, conceptual models have been part of the hydrological literature, for an even longer period, and are presented as an alternative to physically-based models. They do not take into account the detailed geometry of catchments and the small-scale variabilities; rather they consider the catchment as an ensemble of interconnected conceptual storages. In particular, they do not explicitly include any laws of physics, which purportedly underlie physically-based models.

There has been considerable discussion regarding the advantages and disadvantages of both physically-based and conceptual models for the prediction of hydrological responses at the catchment scale (Beven, 1989; Bathurst, 1992; O'Connell and Todini, 1996; Reggiani et al., 1998). Klemes (1983) suggested two diametrically opposite approaches towards the development of theories and models of hydrological response at the catchment scale. The upward or bottom-up approach attempts to combine, by mathematical synthesis the empirical facts and theoretical knowledge available at a lower level of scale into theories capable of predicting the responses at the higher level (Klemes, 1983; Blöschl and Sivapalan, 1995). In terms of the 'upward' development of catchment-scale models, the most recent example is that of Reggiani et al. (1998, 1999, 2000, 2001), who derived the balance equations of mass, momentum, energy and entropy at the scale of a representative elementary watershed (REW), and associated constitutive theory. They went on to develop models of long-term water balance at the REW scale, and runoff routing of river networks, based on the catchment-scale balance equations developed.

The downward or top-down approach of Klemes (1983) strives to find a concept directly at the level or scale of interest (or higher) and then looks for the steps that could have led to it from a lower level or scale. Klemes presents an example of the prediction of monthly runoff in a 39,000 km^2 catchment in Canada. He started with a simple model, found poor fits against observations, and went back to hypothesize the reasons for these poor fits. He consequently included the effect of evaporation, gravity storage and tension storage in steps. At each step he tested the hypothesis by examining the data and was finally able to separate the effects of gravity and tension storages. The work presented in this paper represents one of a series of papers, which have used such a downward or top-down approach for the development of hydrological models (Wittenberg and Sivapalan, 1999; Farmer et al., 2001; Atkinson et al., 2001; Eder et al., 2001). They parallel the work on the upward approach (Reggiani et al., 1998, 1999, 2000, 2001), and it is envisaged that at some point in time, the two approaches will be combined to produce parsimonious models of catchment response which are at the same time physically-based as well as being able to make inferences from observed data through data assimilation exercises.

There are two major themes underlying this paper.

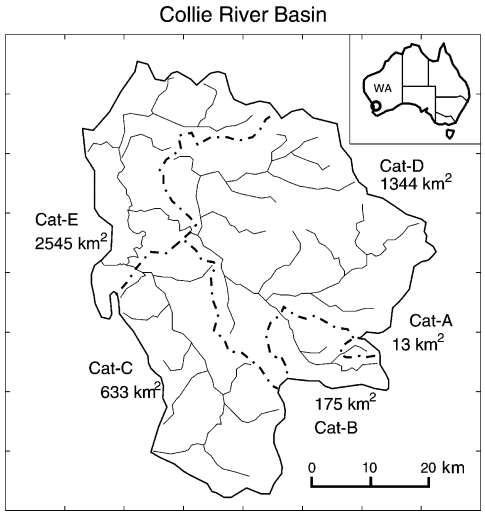

Fig. 1. Location map, stream network and catchment and subcatchment boundaries of the Collie River Basin.

Firstly, the paper presents a new, downward, approach to the art of hydrological model building. Secondly, at every step of the way it addresses the issue of 'what complexity is needed in a conceptual water balance model', along the lines of Jakeman and Hornberger (1993). The latter problem is intimately a management issue tied to the degree of process representation driving the predictions, and must consider the links between model complexity, performance and predictive uncertainty. These are not covered in this paper and are left for future research.

The paper begins with a brief description of the study catchment, and its climate and landscape characteristics. The next section presents the formulation of the annual water balance model, the estimation of parameters, and analysis of required model complexity at this scale. At the annual scale the signature that governs the evaluation of model complexity is the inter-annual variability of water yield. This is followed by the formulation of a monthly water balance model in a similar manner, where the signature plot is the mean monthly variation of runoff (often called the regime curve). The final section presents the formulation of the daily model, where the signature plot used in evaluation of model adequacy is the 'flow duration curve'. Along the way we find an increase in required model complexity, roughly in the following sequence: inclusion of multiple stores, in series and/or in parallel, to reflect the spatial distribution of soil depths, non-linearity in the storage–discharge relationship relating to subsurface runoff, inclusion of a deep groundwater store, and finally streamflow routing in the river network. The models developed are also applied to a range of catchment sizes, and the final model is a spatially distributed one, able to resolve spatial patterns of water yield at the scale of subcatchments.

2. Study catchment

The selected study catchment, shown in Fig. 1, has an area of about 2545 km^2, comprising most of the Collie River Basin located in the south-west region of Western Australia. Hydrological data exists for more than 25 stream gauges (including 16 major subcatchment areas) and there are more than 20 well-distributed rain gauges. We selected a nine-year sequence of daily rainfall and runoff time series (1983–1991) during which most of the gauges were operational. Details of the soils, geology, land formation and vegetation of the Collie catchment are described by Bettenay et al. (1980), and are summarised below.

2.1. Climate and hydrology

The catchment has a Mediterranean climate with cool, wet winters (June–August) and warm to hot, dry summers (December–February). Annual average rainfall decreases from 1100 to 550 mm from west to east, with about 80% of annual rainfall occurring in the May–October period. Annual average potential evaporation measured by the Class A pan also decreases from 1600 to 1400 in a west to east direction. The long-term, areally averaged annual rainfall, potential evaporation and runoff for the Collie catchment are 720, 1500 and 50 mm, respectively.

2.2. Topography, soils and landforms

The valley-side slopes in the western parts of the catchment are about 10–20%. The valleys are deeply incised with local relief of about 50–150 m. These decrease progressively inland. The valley-side slopes are less than 10% in the eastern parts of the catchment, with the valleys being broad and flat and the local

relief rarely exceeding 50 m. The duplex soils consist of predominantly gravelly and sandy lateritic surface soils, 1–10 m thick and of high hydraulic conductivity, overlying deep, kaolinitic sandy clay (about 30 m thick), of much lower hydraulic conductivity. The surface soils (i.e. A horizon soils) have been classified into a number of predominant landform types (Department of Conservation and Environment, 1980). Soil profile data has been collected through extensive drilling carried out for the purposes of estimating soil salt storage. By matching the landform maps with the locations of these measured soil profiles, the distributions of soil depths of the A horizon soils have been estimated for each landform type (Sivapalan and Woods, 1995), and are used in the model development to follow.

2.3. Vegetation

Over uncleared areas, vegetation is dominated by the eucalytptus species *Eucalyptus marginata* and *Eucalyptus calophylla* at the upper and mid slopes, with increasing proportion of *Eucalyptus wandoo* and *Eucalyptus rudis* at the valley floors. The cleared areas are typically sown with annual pastures. The presence of cleared and uncleared areas is assessed from Landsat TM images (visible bands). The interpretation of these satellite images shows that about 30% of the catchment area has been cleared of native vegetation and replaced by annual pasture.

3. Annual water balance model

We assume that the climate is represented by one long rainfall period t_r and a non-rainy period, $\tau - t_r$, where τ is equal to 1 year. Rainfall intensity, p, during the rainy period is assumed constant, equal to the annual rainfall P divided by the duration t_r. Potential evaporation e_p (assumed uniform throughout the year) is equal to the annual potential evaporation E_p divided by 365 days. The model allows for variability of P and E_p between years, but assumes that t_r remains constant, as a first approximation.

Inspired by Manabe (1969) and Milly (1994), the model initially conceptualizes the catchment response in terms of a single 'bucket', with a finite storage capacity estimated from spatially averaged soil depth and porosity. Annual rainfall is partitioned into evaporation and surface runoff. Evaporation includes interception loss from plant canopies at the land surface, and combined evaporation and transpiration taken out of the soil water held within the bucket. Surface runoff is generated when soil water storage in the bucket exceeds its storage capacity.

3.1. Water balance equation

The general volumetric water balance per unit surface area over a short time period (much shorter than a year), for the single bucket model, is given by

$$\frac{ds(t)}{dt} = p(t) - q_{se}(t) - e(t) \tag{1}$$

where $p(t)$ is the precipitation intensity, $q_{se}(t)$ is the saturation excess runoff rate, $e(t)$ is the evaporation rate, and $s(t)$ is the volume of soil water storage. The outflows, $q_{se}(t)$ and $e(t)$, appearing in Eq. (1) are described as functions of soil water storage $s(t)$.

$$q_{se} = (s - S_b)/\Delta t \qquad \text{if} \qquad s > S_b \tag{2a}$$

$$q_{se} = 0 \qquad \text{if} \qquad s \le S_b \tag{2b}$$

$$e = \frac{s}{S_b} e_p \tag{3}$$

where $S_b = D\phi$ is the single bucket's storage capacity, with D being the average soil depth, ϕ the average porosity, and Δt is the time step (which in this case is 1 day).

The water balance model given by Eqs. (1)–(3), is applied using rainfall and potential evaporation time series, constructed over many years using their annual totals, as explained before. To avoid specification of the unknown initial condition at the beginning of simulations, we assume that the final value of soil water storage at the end of the complete simulation cycle (after multiple number of years) is equal to the initial value, and these values are obtained by iteration. This is a reasonable assumption for the climate of Western Australia, since there is very little carry-over of soil moisture between years.

3.2. Parameter estimation

The parameters needed for the annual water balance are as follows:

Climate inputs P, t_r, E_p, i

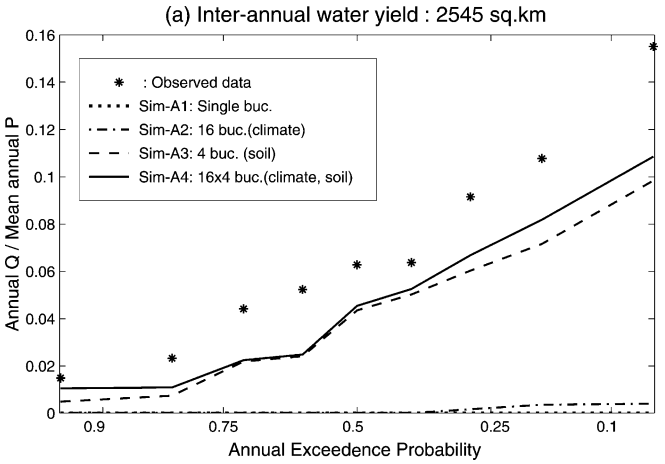

Fig. 2. Comparison of observed and simulated annual water yields for the first type of models, based on annual input data for the entire Collie catchment, 2545 km^2.

Soil parameters D, ϕ

The model uses two time series of climatic inputs, namely, rainfall intensity and potential evaporation. Rainfall rate, p, is generated from observed annual rainfall, P, divided by number of rainy days per year, t_r. Potential evaporation, e_p, is generated from observed annual potential evaporation divided by number of days in each year (mostly 365). The interception loss, i, expressed as a proportion of rainfall, is assumed to be 10% of rainfall for all years; average interception for forested areas is about 13% and 70% of total area is now forested. Bucket capacity, S_b, for the Collie catchment was estimated to be 1200 mm, based on the estimated average depth of the upper layer of the duplex soils, 3 m, and a porosity of 0.4 (sandy loam).

3.3. Required model complexity

The downward approach starts with the simplest model structure, consisting of a single bucket, assuming that the entire Collie catchment is homogeneous with uniform climate and soil depth (Sim-A1). The next level of complexity is to represent the catchment in terms of multiple buckets that act in parallel. In this case we assume that all of the buckets are of the same size (i.e. uniform soil depth), but account for the spatial variability of rainfall only (Sim-A2), while keeping all of the other properties constant as well. In this case we used 16 buckets, which is the same as the number of subcatchment scale rainfall zones that we have adopted, based upon analysis of gauged rainfall data across the catchment, to adequately capture the spatial variability of rainfall. In the next step, the multiple-bucket model is used to account for spatial variability of soil (i.e. bucket capacity, S_b) while neglecting the variability of climatic inputs and other catchment characteristics (Sim-A3). Based on limited data available, we chose four buckets of sizes $S_b = 200$, 800, 1300 and 2500 mm, to represent the spatial distribution of soil depths. In the final step, the multiple-bucket model is used to include spatial variability of annual rainfall totals *and* the bucket capacity ($16 \times 4 = 64$ buckets), with all remaining parameters being kept constant (Sim-A4). Each of these models is applied to simulate the annual water balance of the catchment. The results are presented in terms of frequency plots, relating the estimated or measured annual runoff yield to its annual exceedance probability, which is defined as the probability that the given annual runoff total will be exceeded in any given year. We call this the inter-annual variability plot of annual water yield, which is the first signature that we will use to assess model predictions.

Fig. 2 presents a comparison of the inter-annual variability plots between each of the simulation steps described above, and against that estimated from measured streamflow data. Sim-A4, which includes spatial variability of both annual rainfall and soil depths, already provides a good match to the observed

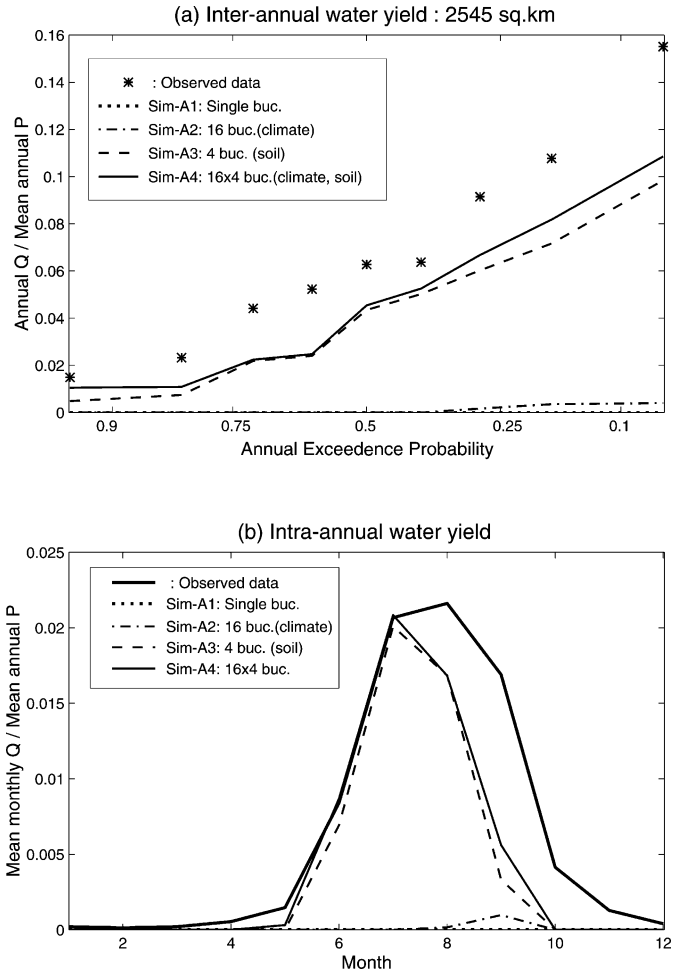

Fig. 3. Comparison of observed and simulated water yields from the first type of models, based on monthly input data for the Collie catchment, 2545 km^2: (a) inter-annual variability, (b) intra-annual (mean monthly) water yield.

inter-annual variability plot. Sim-A3, which includes only the spatial variability of soil depths, gives as good a fit even though it does not include spatial variability of rainfall. The inclusion of rainfall variability alone (Sim-A2) does not account for the observed behaviour. Thus, the main conclusion that can be drawn is that in this catchment the spatial variability of soil depths is much more important for the annual water balance than the spatial variability of rainfall, despite the large spatial variability of rainfall, with mean annual rainfall decreasing from about 1200 mm in the west to about 550 mm in the east. The single, lumped model considered above is clearly inadequate to capture the annual water balance, under any circumstances.

4. Monthly model formulation

Without any change to the number of parameters or to model complexity, the different versions of the model formulated in Section 3 were next applied with monthly climate inputs. The difference this time is that we consider seasonal variability of climatic inputs, but in a simple way. Each month is divided into a wet (rainy) period and a dry period. The rainfall intensity during the rainy period and the potential evaporation over the entire month are assumed to be constant for each month. Multi-year time series of rainfall intensity and potential evaporation are then formed from observed monthly totals of

rainfall divided by the average number of rainy days per month, and of monthly potential evaporation divided by the number of days in each month. For these monthly models, intra-annual (i.e. mean monthly or seasonal) variability of the runoff yield is now included as a new signature of runoff variability, to add to the inter-annual variability of annual yield considered before. As before, the unknown initial condition of each bucket (for multiple bucket models) is estimated iteratively by equating it to the value at the end of a multi-year simulation.

The results from the application of the model with the monthly climatic data are presented in Fig. 3. In the case of inter-annual variability, results for the model configurations, Sim-A1 to Sim-A4, are very similar to the corresponding results obtained previously with annual climatic data (Fig. 2), except for a slight under-prediction of annual yield in all years. On the other hand, the intra-annual (i.e. mean monthly) variability of runoff yield is not predicted well, even with the best possible model configuration (64 buckets in parallel, to account for spatial variability of rainfall and soil depth). Comparison with observed data suggests a significant under-prediction of monthly runoff between July and December for this model, suggesting a need to introduce a delay mechanism in the runoff generation process.

In response to the above results, the building block component (individual buckets) of the previous water balance model is then extended through the introduction of additional processes. Runoff is now separated into two components: a delayed subsurface runoff, q_{ss}, when soil moisture storage in the bucket exceeds a field capacity threshold; and, as before, the saturation excess runoff, q_{se}, when the bucket capacity is exceeded. In addition, in order to account for the effects of heterogeneity of vegetation cover, which is a reality in this catchment due to considerable clearing of native forests for agriculture, total evapotranspiration is partitioned into bare soil evaporation, e_b, and transpiration, e_v. Total evapotranspiration is estimated by weighting each of these two rates by the fractions of the catchment area covered by bare soil or shallow-rooted crops, and by deep-rooted native vegetation, respectively.

4.1. Water balance equation

The new water balance equation for the revised, single bucket model is then given by:

$$\frac{ds(t)}{dt} = p(t) - q_{ss}(t) - q_{se}(t) - e_b(t) - e_v(t) \tag{4}$$

The outflows from the bucket appearing on the RHS of Eq. (4) are described as functions of soil water storage, s, and are described below.

4.1.1. Subsurface runoff

$$q_{ss} = \frac{s - s_f}{t_c} \quad \text{if} \quad s > s_f \tag{5a}$$

$$q_{ss} = 0 \quad \text{if} \quad s < s_f \tag{5b}$$

where s_f is the soil-water storage at field capacity, and t_c is a catchment response time with respect to subsurface flow. The threshold storage, s_f, is assumed to be equal to $s_f = f_c D$, where f_c is the soil's field capacity, and D is the average soil depth. The reason for the use of the field capacity is that often when the moisture content is less than the field capacity, capillary forces are larger than those of gravity and drainage is prevented. The response time $t_c$is estimated by applying Darcy's law to an idealized, triangular representation of the groundwater aquifer within a planar hillslope, assuming that the hydraulic gradient can be approximated by the slope of the ground surface. This gives:

$$t_c = \frac{L\phi}{2K_s \tan\beta} \tag{6}$$

where ϕ is average soil porosity, L is average hillslope length, $\tan\beta$ is average ground surface slope, and K_s is the average saturated hydraulic conductivity.

4.1.2. Saturation excess runoff rate

$$q_{se} = (s - S_b)/\Delta t \quad \text{if} \quad s > S_b \tag{7a}$$

$$q_{se} = 0 \quad \text{if} \quad s < S_b \tag{7b}$$

where S_b, as before, is the bucket's soil moisture storage capacity, given by $S_b = D\phi$, and Δt is the time step (1 day here).

Table 1
Spatially averaged catchment characteristics: Collie catchment

Parameter	Value	Units
L	300	m
$tan\beta$	0.1	–
ϕ	0.4	–
K_s	10	m/day
D	3.0	m

4.1.3. Bare soil evaporation rate

$$e_b = \frac{s}{t_e} \tag{8}$$

$$t_e = \frac{S_b}{(1-M)e_p} \tag{9}$$

where t_e is a characteristic time scale associated with bare soil evaporation, estimated using Eq. (9), where e_p is the potential evaporation rate, and M is the fraction of forest vegetation cover ($0 < M < 1$).

4.1.4. Transpiration rate

$$e_V = Mk_V e_p \quad \text{if} \quad s > s_f \tag{10a}$$

$$e_V = \frac{s}{t_g} \quad \text{if} \quad s < s_f \tag{10b}$$

$$t_g = \frac{s_f}{Mk_V e_p} \tag{11}$$

where t_g is a characteristic time scale associated with transpiration and, following Eagleson (1978), k_V is a plant transpiration efficiency (generally set equal to 1).

Parameter M is used to partition total evaporation into bare soil evaporation and transpiration. Bare soil evaporation is a proportion of e_p depending on the ratio of s and S_b. When s is larger than s_f, transpiration rate is at a maximum rate equivalent to e_p. We allow it to be higher than e_p for some tree species by allowing k_v to be larger than 1. When s falls below s_f, transpiration rate is a fraction of e_p as a function of soil moisture storage s.

4.2. Parameter estimation

The parameters for this extended water balance model are grouped into the following categories.

Table 2
Spatially averaged parameters for the second type of models (monthly model)

Parameter	Value	Units
S_b	1200	mm
f_c	0.16	–
t_c	60	Days
M	0.7	–
k_v	1.2	–
i	10	%

Monthly climate parameters: P_m, t_{rm}, E_{pm}, i_m; $\forall m = 1,\ldots,12$.
Soil and topographic parameters: D, ϕ, f_c, L, $\tan\beta$, K_s
Vegetation properties: M, k_v

The monthly climate parameters are obtained from observed monthly rainfall and potential evaporation. The topographic and soil parameters for the Collie catchment are presented in Table 1. The model parameters t_c can be estimated from the catchment characteristics given in Table 1 using Eq. (6). Table 2 summarizes model parameters estimated for the total catchment. Note that the magnitudes of the physical characteristics reported in Table 1 are approximate averages of properties that generally exhibit enormous spatial variability. For example, measured point values of K_s in a small 0.94 km^2 subcatchment (Wights) were found to be in the range 0.2–22.7 m/day (Sharma et al., 1987b). With variabilities of such extent, estimation of catchment-scale parameter values is always subject to considerable uncertainty, with the consequent uncertainty of model predictions. This issue is discussed in some depth, and in a similar context, in Atkinson et al. (2001). The model is also implemented without any runoff routing because the travel time of water flows in this catchment is of the order of a few days which is much shorter than the monthly and annual time scales at which the model is being evaluated at this stage of development.

4.3. Model complexity analysis

Similar to Section 3.3, a model complexity analysis was performed in five steps, with respect to this second type model (denoted Sim-M1 to Sim-M5), to investigate climate, soil and vegetation controls on runoff variability. Fig. 4 presents a comparison of

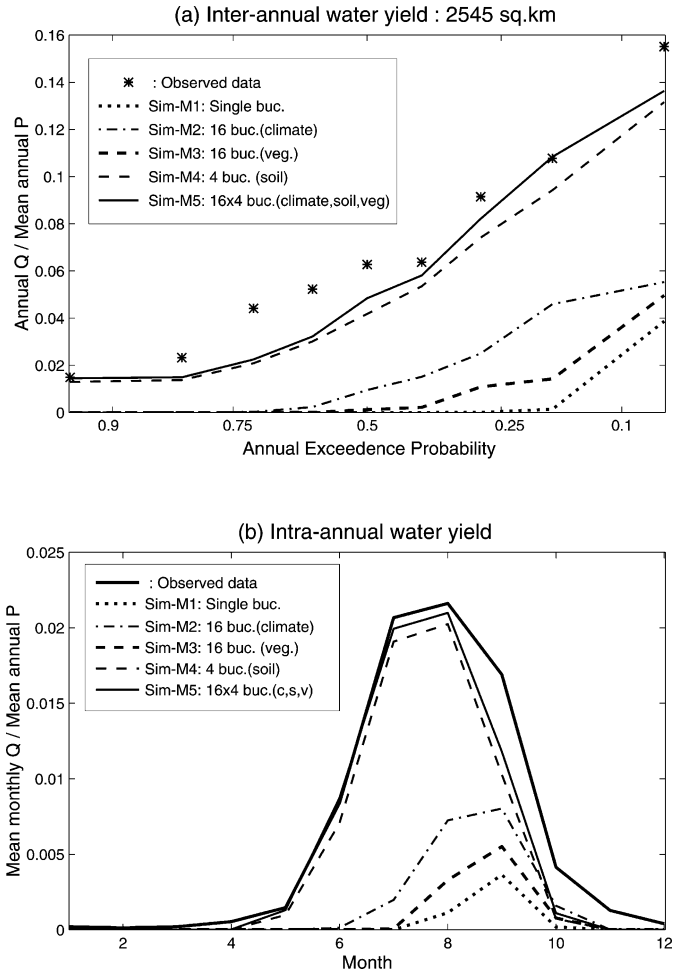

Fig. 4. Comparison of observed and simulated water yields from the second type of models based on monthly input data for the Collie catchment, 2545 km^2: (a) inter-annual variability, (b) intra-annual (mean monthly) water yield.

the inter-annual and intra-annual (mean monthly) variabilities of runoff yield between each of the simulation steps (Sim-M1 to Sim-M5), and against observed data. The simulated results from the fifth step (Sim-M5, 64 buckets) demonstrate that the new model, when operated with parallel multiple buckets, is able to capture the observed inter-annual and intra-annual variabilities better than Sim-A4 in Fig. 3, the most complex model considered in Section 3.3 (i.e. annual model). This confirms that delayed subsurface runoff, along with a separate treatment of transpiration and bare soil evaporation, are necessary for accurate predictions, especially of the intra-annual (mean monthly) variability of runoff. In particular, the inclusion of subsurface flow in what is often called a 'leaky bucket' model has enabled a more realistic prediction of the delays seen in observed monthly flow data.

5. Daily model formulation

Further testing of the second type storage model presented in Section 4, and operated there using monthly climatic data, was next carried out to ascertain whether the process complexity in this model is sufficient to make predictions at daily time step. If found inadequate, the objective then is to determine what additional process complexity

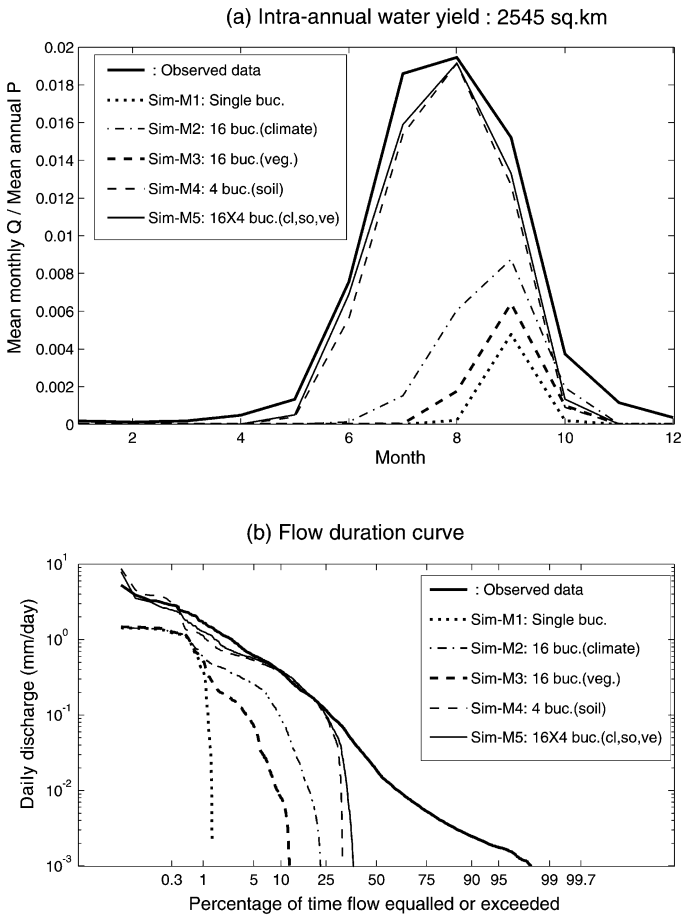

Fig. 5. Comparison of observed and simulated water yields from the second type of models based on daily input data for Collie catchment, 2545 km^2: (a) intra-annual (mean monthly) water yield, (b) flow duration curve (based on daily flows).

needs to be included to match observed daily runoff data.

We introduce the flow duration curve as a third 'signature' of runoff variability, in addition to the inter-annual and intra-annual variability signatures used before. The flow duration curve is a plot of the magnitude of daily flow against the probability that it will be exceeded on any given day; in fact, it is an expression of the cumulative distribution function based on daily flows, and is different from the inter-annual variability plot previously used, in that it represents the longer term random variability of stream-flows. Fig. 5 presents a comparison of the simulation results for the five different simulation steps investigated in Section 4, but this time using actual daily measurements of rainfall intensity and potential evaporation. Model complexity is assessed in terms of how the models are able to reproduce the two signatures of runoff variability: mean monthly variation of runoff and the flow duration curve (based on daily flows).

Results presented in Fig. 5 for the entire Collie catchment show that the intra-annual variabilities are similar to what were obtained before in Section 4. Good fits to observed data are obtained [Fig. 5(a)], with the multiple-bucket model that includes spatial variability of soils, climate and vegetation. However, a good match to the flow duration curve is not obtained, with low flows at the tail end of the flow duration curve being significantly underestimated.

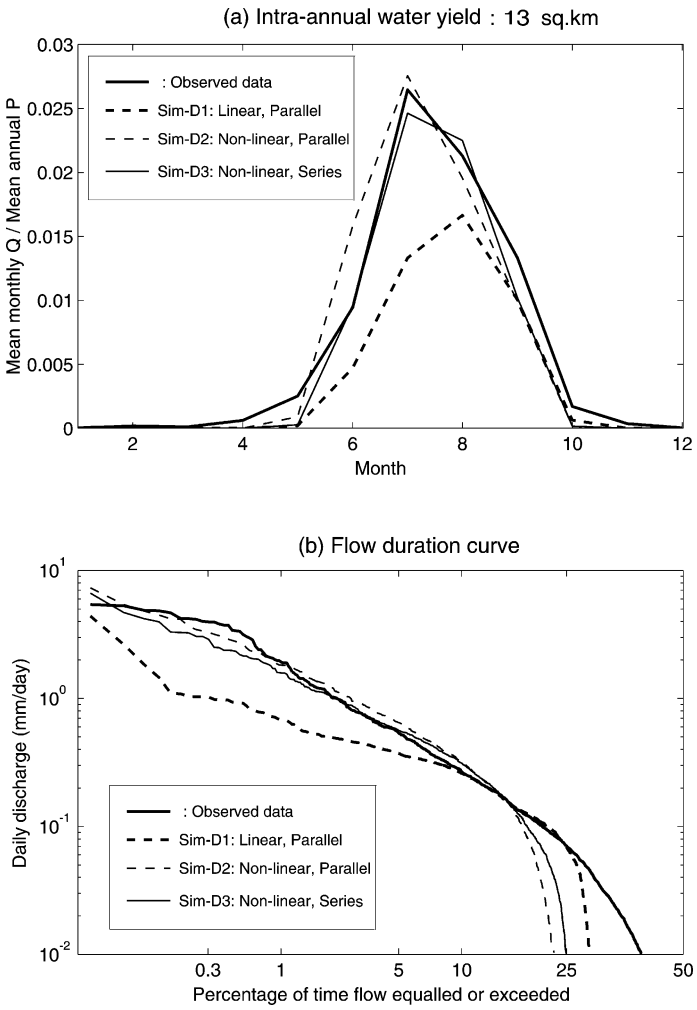

Fig. 6. Comparison of observed and simulated water yields between three simulation steps, for the third type models (with daily data) for subcatchment Cat-A, 13 km^2. Sim-D1: linear storage–discharge relationship and multiple buckets in parallel, Sim-D2: non-linear storage–discharge relationship and multiple buckets in parallel, Sim-D3: non-linear storage–discharge relationship and multiple buckets in series. (a) Intra-annual (mean monthly) water yield, (b) flow duration curve (daily flows).

Measured runoff data suggests that the Collie River flows almost throughout the year, yet the current model type generates runoff, at most, for 6 months only [Fig. 5(b)]. This suggests a need for additional complexity to better simulate low flows. This will be discussed later.

To examine the adequacy of the previously described model for regional predictions and to catchments of different sizes, it was next applied to a 13 km^2 subcatchment (denoted Cat-A and shown in Fig. 1), initially using the same model structure and parameters, but gradually evolving to a third-type, more complex model. The results of the first simulation (Sim-D1) are presented in Fig. 6 (denoted as step 1: linear and parallel buckets). They show that the predictions are worse (mainly under-predictions), for both signatures, than the corresponding ones for the Collie catchment as a whole. Apart from the problem of low flow prediction, the results suggest, at the very least, that the catchment averaged parameters for the Collie as a whole are not adequate for the smaller subcatchment. This can be addressed by adjusting

Table 3
Estimated parameters for the third type of models (daily model) for five different subcatchments

List of parameters	Cat-A 13 (km^2)	Cat-B 175 (km^2)	Cat-C 633 (km^2)	Cat-D 1344 (km^2)	Cat-E 2545 (km^2)
Model structure					
Number of subcatchment	1	8	27	66	116
Number of serial buckets in each subcatchment	20	20	20	20	20
Storage–discharge relationship					
a (mm$^{0.5}$ day$^{0.5}$)	14	15	15	15	15
b	0.5	0.5	0.5	0.5	0.5
Soil properties					
Measured D (m)	2.45	2.40	2.60	2.40	2.50
Adjusted D (m)	–	–	–	2.95	3.00
ϕ	0.4	0.4	0.4	0.4	0.4
f_c	0.16	0.16	0.16	0.16	0.16
Vegetation					
M	0.5	0.2–0.9	0.1–1.0	0.0-1.0	0.0–1.0
k_v	1.2	1.2	1.2	1.2	1.2
i (forest, %)	10	10	12–15	10-13	10-15
Deep groundwater					
λ	0.2	0.2	0.2	0.2	0.2
Stream routing					
Stream velocity (km/d)	15	15	15	15	15

the model parameters for this subcatchment to more appropriately reflect local characteristics, but is avoided at this stage because we do not have soils data specific to this subcatchment.

5.1. Non-linear storage discharge relationship

In response to these deficiencies of the above model operated at the daily time scale, the first generalisation we make is to modify the storage–discharge relationship for subsurface flow from a linear to non-linear one. The linear storage–discharge relationship, Eq. (5), with the single parameter, t_c, is replaced with the following non-linear relationship with two parameters a and b:

$$q_{ss} = \left[\frac{s - s_f}{a}\right]^{\frac{1}{b}} \quad \text{if} \quad s > s_f \tag{12a}$$

$$q_{ss} = 0 \quad \text{if} \quad s < s_f \tag{12b}$$

5.1.1. Parameter estimation

In this paper, we estimate the parameters a and b through recession analyses carried out on measured streamflow data prior to the development of the model. To see the connection, first consider the continuity equation, Eq. (4), for the subsurface store, in the aftermath of rainfall events, i.e. rainfall is zero, and assuming negligible surface runoff and evaporation loss (these are reasonable assumptions for the Collie catchment), and Eq. (4) then simplifies to $ds/dt = -q_{ss}$. Furthermore, making a quasi-steady state approximation, we assume that $Q = q_{ss}$, where Q is the discharge in the river normalised by the catchment area. Combining these with Eq. (12) leads to (Wittenberg, 1999; Wittenberg and Sivapalan, 1999):

$$\frac{dQ}{dt} = -\frac{Q^{2-b}}{ab} \tag{13}$$

and

$$Q_t = Q_0\left[1 + \frac{(1-b)Q_0^{1-b}}{ab}t\right]^{\frac{1}{b-1}} \tag{14}$$

where Q_0 is observed discharge at the starting point of the recession curve, and Q_t is observed discharge at time t. Using Eq. (14), the values of a and b can be obtained from best fits to the observed recession curves by an iterative least squares fitting method (Wittenberg, 1994; Atkinson et al., 2001).

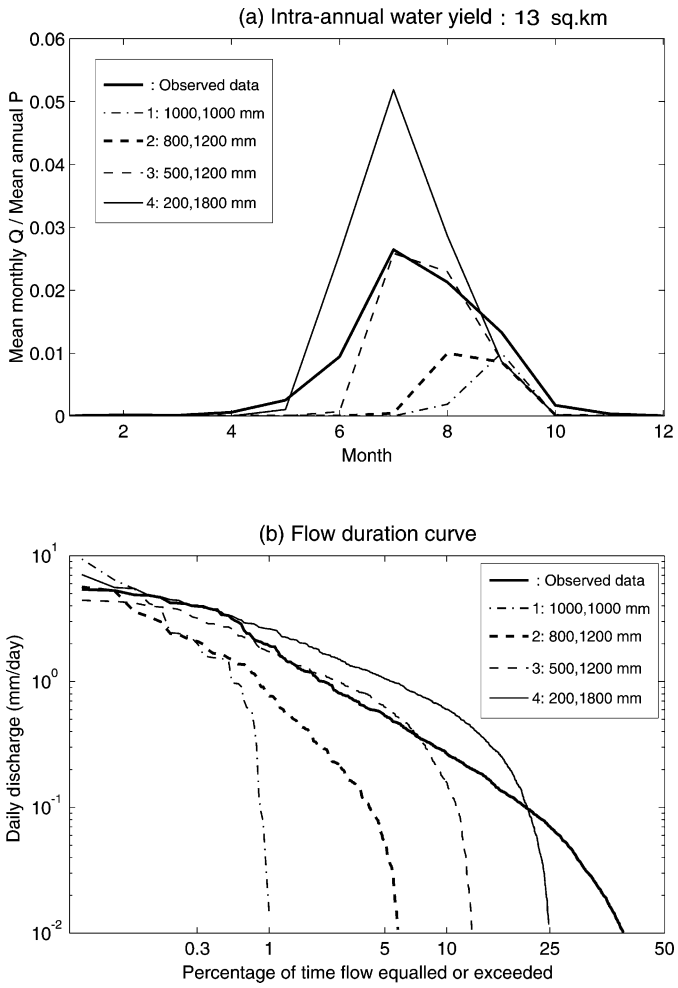

Fig. 7. Comparison of observed and simulated water yields between four simulation steps involving two buckets (in series) of sizes: (1) 1000, 1000 mm, (2) 800, 1200 mm (3) 500,1500 mm, (4) 200, 1800 mm, for the third type of models with non-linear storage–discharge relationship and daily input data for the subcatchment Cat-A, 13 km^2. (a) Intra-annual (mean monthly) water yield, (b) flow duration curve (daily flows).

In this semi-arid region, the influence of evaporation is strong, and gives rise to different recession parameters in summer and winter, for example, which cannot be ignored in the recession analysis. Wittenberg and Sivapalan (1999) have presented an iterative scheme to separate the influences of evaporation from that of subsurface drainage. A similar technique was used to estimate the parameters *a* and *b* in the Collie catchment and many of its subcatchments, and are presented in Table 3. Empirical analysis, supported by previous theoretical studies, suggest that the parameter *b* falls around 0.5, and was here taken to be a constant for the sake of simplicity.

5.1.2. Effect of non-linearity in small subcatchment

The effect of the introduction of non-linearity in the subsurface runoff generation is examined through simulation again with our third-type model (Sim-D2) for Cat-A (13 km^2), with parameters estimated as described above. The results are again presented in Fig. 6 (Step-2: non-linear, parallel buckets). A comparison of the results of Sim-D1 and Sim-D2 reveals that the introduction of non-linearity has (1) significantly increased the magnitude of annual and mean monthly runoff yields (giving a good match to observed data), and (2) has increased the magnitude of peak flows (giving a good match to the high end of the

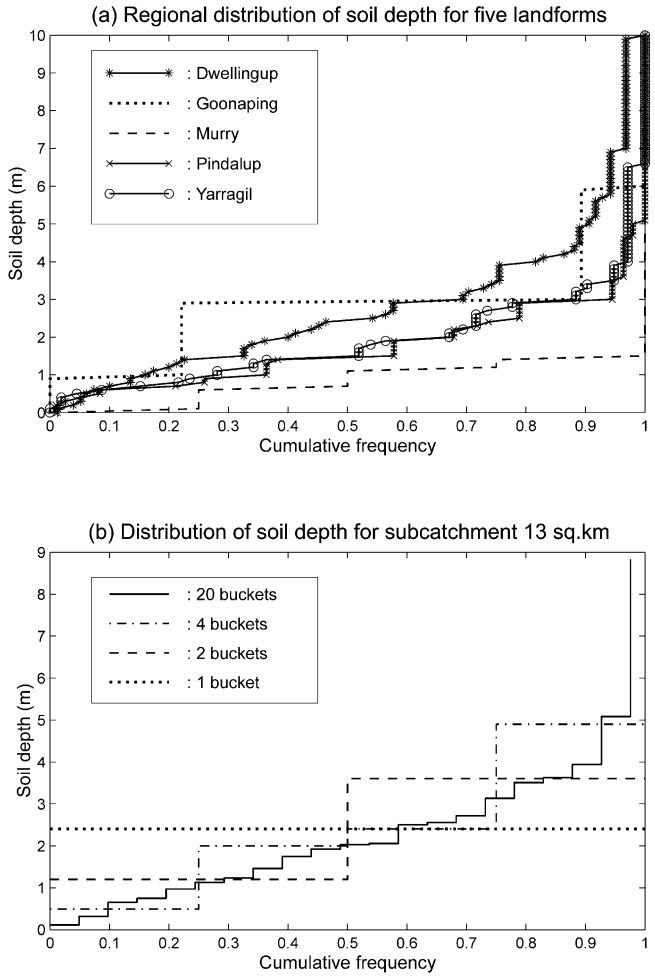

Fig. 8. (a) Regionalized cumulative distribution of soil depths for five typical landforms in the south-west of Western Australia. (b) Distribution of soil depths for subcatchment Cat-A (13 km^2) based on combinations of different landform types, approximate distributions for four different bucket configurations.

flow duration curve). This result indicates that for peak flows the catchment averaged parameters are sufficient and it is not necessary to estimate soil storage parameters specific to this subcatchment. However, it only makes a marginal impact on the magnitude of low flows.

5.2. Multiple buckets in series

So far, the multiple bucket formulations have only considered buckets in parallel. However, there is a possibility that this may not be adequate for small catchments, because it ignores the interactions between different stores. Thus we considered the applicability of, and the need for, buckets which are 'in series', whose subsurface runoff contribution is generated from a store which is common to all buckets. Fig. 6 also shows a comparison of the results from Sim-D2 (non-linear, parallel) and Sim-D3 (non-linear, series), with the same configuration of bucket sizes used before. It shows that the 'serial bucket' model produces a better flow duration curve than the parallel bucket one, with no change to the other signature plot. Especially, the use of multiple buckets in series has lifted the flow duration curve in the range of high flows closer to the observed.

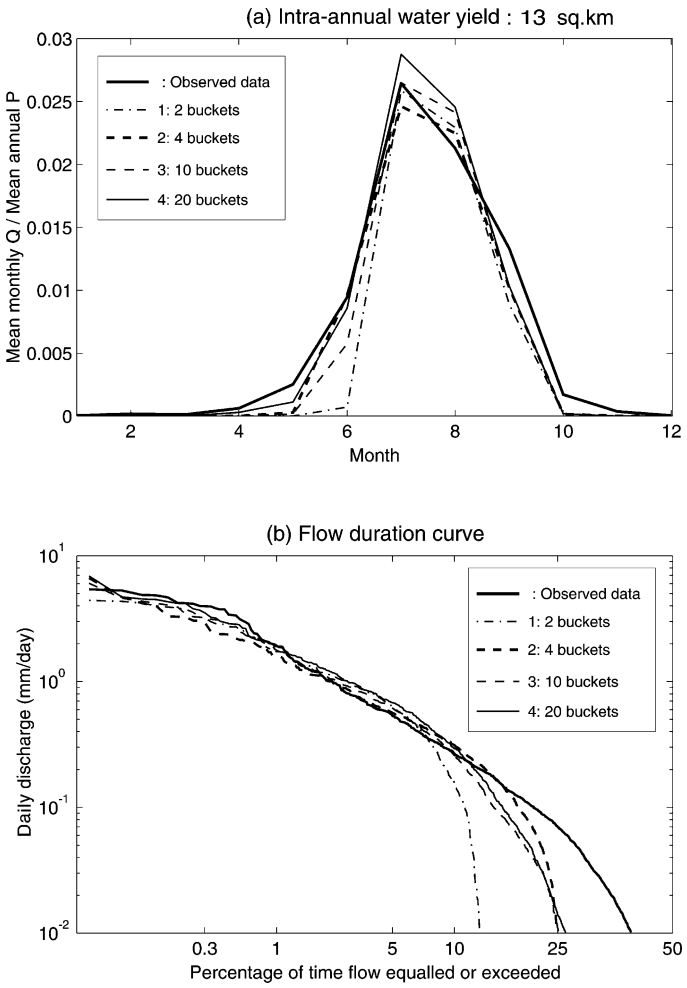

Fig. 9. Comparison of observed and simulated water yields between four simulation steps involving increasing number of buckets: (1) two buckets, (2) four buckets (3) 10 buckets (4) 20 buckets, using the third type of models, multiple buckets in series and non-linear storage–discharge relationship, with daily input data for the subcatchment Cat-A (13 km^2). (a) Intra-annual (mean monthly) water yield, (b) flow duration curve (daily flows).

5.3. Distribution of soil depths

It has been repeatedly demonstrated in this paper that the distribution of soil depths is an important determinant of water yield, whereas the choice of bucket sizes has been so far quite arbitrary. To further investigate the effects of the variability of soil depths in small catchments, we applied the new non-linear storage model, with just two buckets acting in series, to the small subcatchment, Cat-A (13 km^2), while preserving the same average bucket capacity. The results are presented in Fig. 7, and show that the range of bucket capacities makes a significant impact on both signatures of runoff variability, highlighting the need to estimate the soil depth distribution accurately to ensure the soundness of predictions.

The distribution of soil depths, converted to distribution of storage capacity, can in principle be estimated from available soil maps and soil profile data. Knowing the spatial extent of different landforms within a subcatchment, and the empirical distribution of soil depths available for each landform type, a composite distribution of soil depths can be estimated as the area-weighted combination of the

distribution of soil depths for individual landform types. This has been previously described in detail by Sivapalan and Woods (1995). Fig. 8(a) shows the regionalised distribution of soil depths for different landform types in Western Australia, which was based on extensive drilling in the region, and Fig. 8(b) shows the composite soil depth distribution for subcatchment Cat-A (13 km^2) based on the following area weightings: 60% Dwellingup and 40% Pindalup. Different possible configurations of bucket sizes, ranging from just two buckets to 20, designed to approximate this composite distribution, are also presented in Fig. 8(b).

We then applied this revised (third-type) water balance model (multiple buckets in series, non-linear storage–discharge relationship) to subcatchment Cat-A (13 km^2), for the various configurations of bucket sizes presented in Fig. 8(b). The results are presented in Fig. 9. They demonstrate that models with the larger number of buckets do provide better fits to the signature plots, but the improvements appear to be marginal beyond four buckets. Indeed, even with 20 buckets, the flow duration curve still remains under-predicted for very low flows.

5.4. Deep groundwater storage

The ability to predict extended low flows is an important attribute required in long-term water balance models in this region. Yet, as noted before, the models considered so far have failed to adequately capture the tail of the flow duration curve. Extensive sensitivity analyses, with respect to the parameter values and bucket configurations, were carried out but did not identify an easy solution to this problem.

The presence of duplex soils, and empirical evidence regarding the occurrence of a perched groundwater system as well as a deeper, more permanent groundwater system, suggested to us that the introduction of a deeper groundwater store may help improve low flow predictions. A number of other conceptual models that have been developed for catchments in this region have incorporated a deeper groundwater store to good effect. Examples of these are the Large Scale Catchment Model or LASCAM (Sivapalan et al., 1996a,b), and the Generalized Surface Infiltration Baseflow Model or GSFB (Boughton, 1984; Ye et al., 1997).

The structure of the model was therefore revised to include a coupling to an underlying deep groundwater store. The water balance for the deep groundwater store is given by

$$\frac{ds_g(t)}{dt} = \lambda q_{ss}(t) - q_{sg}(t) \tag{15}$$

$$q_{sg}(t) = \left[\frac{s_g}{a}\right]^{\frac{1}{b}} \tag{16}$$

$$q_{total} = (1-\lambda)q_{ss} + q_{sg} + q_{se} \tag{17}$$

where $s_g(t)$ is the volume of deep groundwater storage, q_{ss} as before is the subsurface runoff rate, λ is the proportion of the subsurface runoff percolating to the deep groundwater store, q_{sg} is groundwater runoff and q_{total} is total water yield from the catchment.

The average annual deep groundwater recharge in the Salmon catchment, a subcatchment located just downstream of the Collie catchment, was estimated by Stokes (1985) and Johnston et al. (1983) to be 25–30 mm/year or about 20% of the annual subsurface runoff. Based on this preliminary evidence, we assume for simplicity that recharge to the deep groundwater store is 20% of the subsurface flow ($\lambda = 0.2$) from the perched aquifer above. This ratio is further assumed to be spatially constant across the entire catchment, as a first approximation. Similarly, the parameters a and b relating to the discharge from the deeper aquifer are also assumed to be equal to the corresponding values for the perched aquifer, again for simplicity. These are somewhat crude assumptions, but are sufficient for the purposes of this paper.

The results of the application of this enhanced (third-type) water balance model (non-linear, multiple buckets in series, deeper groundwater store) to subcatchment Cat-A are presented in Fig. 10. They show that the addition of the deeper groundwater store has lifted the lower tail of the flow duration curve, and gives a reasonably good fit to the flow duration curve based on observed flows. The final set of parameters of the enhanced model for subcatchment Cat-A is presented in Table 3.

5.5. Distributed model of catchment water balance

So far in this paper, starting with the simplest of models, we have gradually and systematically

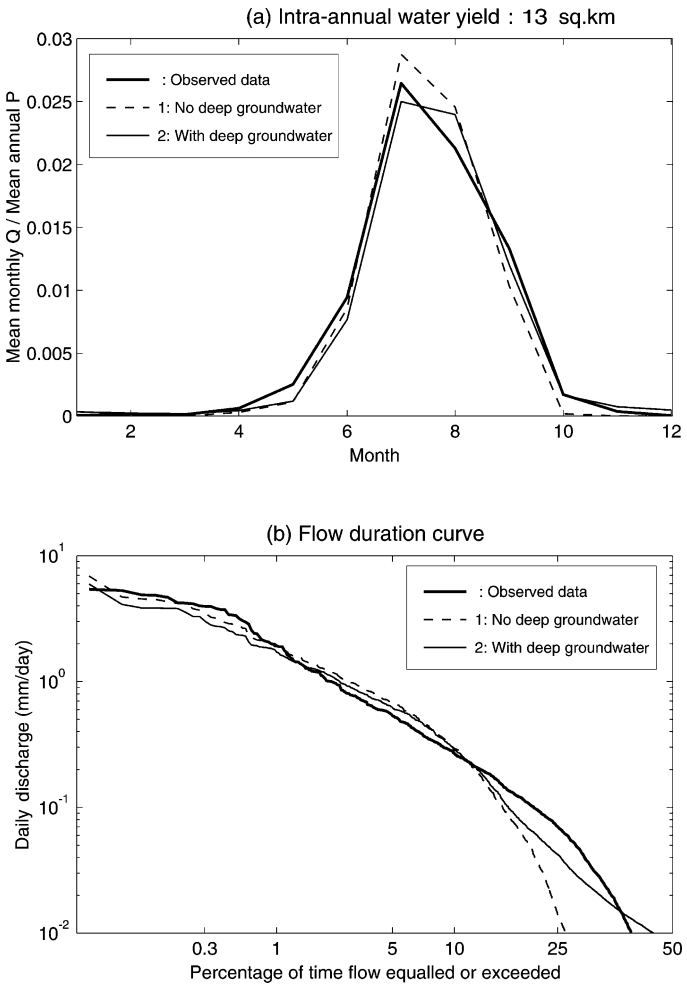

Fig. 10. Comparison of observed and simulated water yields between two simulation steps of the third-type model: (1) no deep groundwater store and (2) with deep groundwater store, using the third type of models for subcatchment Cat-A (13 km^2). (a) Intra-annual (mean monthly) water yield, (b) flow duration curve (daily flows).

included additional processes in steps, to reproduce signatures of runoff variability at the annual, monthly and daily time scales. The processes and complexities added include, in order, multiple buckets based on empirical soil depth distributions, delayed subsurface flow, non-linearity of the storage–discharge relationship, and the deep groundwater store. We have tested the effects of many of these additions in a small subcatchment.

In the next step, we will apply the latest model configuration (multiple non-linear buckets in series with a deep groundwater store) as the building block of a distributed model of the entire Collie catchment. The catchment is divided into 116 subcatchments based on topography and the stream network. Each subcatchment has its own input data with respect to climate, soils, and vegetation (and the resulting estimate of daily interception loss). Interception for forested areas is assumed to vary between 10% in the eastern end of the catchment to 15% in the western end, as suggested by Williamson et al. (1987). In our distributed model, the different subcatchments are assumed to respond to the climate inputs independently (i.e. they act in parallel), and the generated runoff is then routed down the stream network. For a catchment of this size, accurate prediction of the

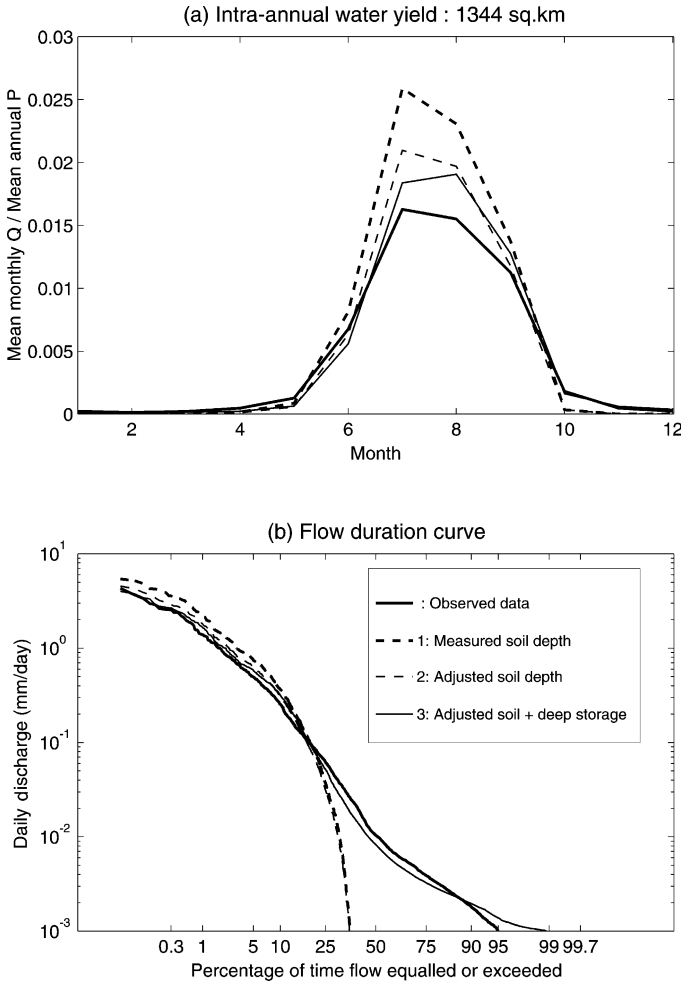

Fig. 11. Comparison of observed and simulated water yields between three simulation steps of the third-type model: (1) measured soil depth without deeper groundwater, (2) measured soil depths with deep groundwater store, and (3) adjusted soil depths with deep groundwater store, using the third type of models for the subcatchment, Cat-D (1344 km^2): (a) intra-annual (mean monthly) water yield, (b) flow duration curve (based on daily flows).

daily runoff variability does require a routing component to the model, and is described below.

5.5.1. Stream network routing

The routing model is based on a constant stream velocity algorithm developed by Viney and Sivapalan (1995). It assumes that the runoff volume from upstream subcatchments enters the stream channel uniformly in time throughout the day, and that runoff from the adjacent hillslopes enters the stream uniformly in time and uniformly in space along the channel length. Using a single optimizable parameter, a stream velocity (v), assumed constant in space and time, the model calculates the volume of runoff passing out of each subcatchment in each time step, and the in-stream runoff volume that has not yet reached the subcatchment outlet. This model, unlike the Muskingum–Cunge model, does not require knowledge of the channel cross-section, and does not introduce any other unknown parameters.

5.5.2. Simulation results from selected subcatchments

Results of the application of the distributed, large catchment-scale model are presented in Figs. 10–12,

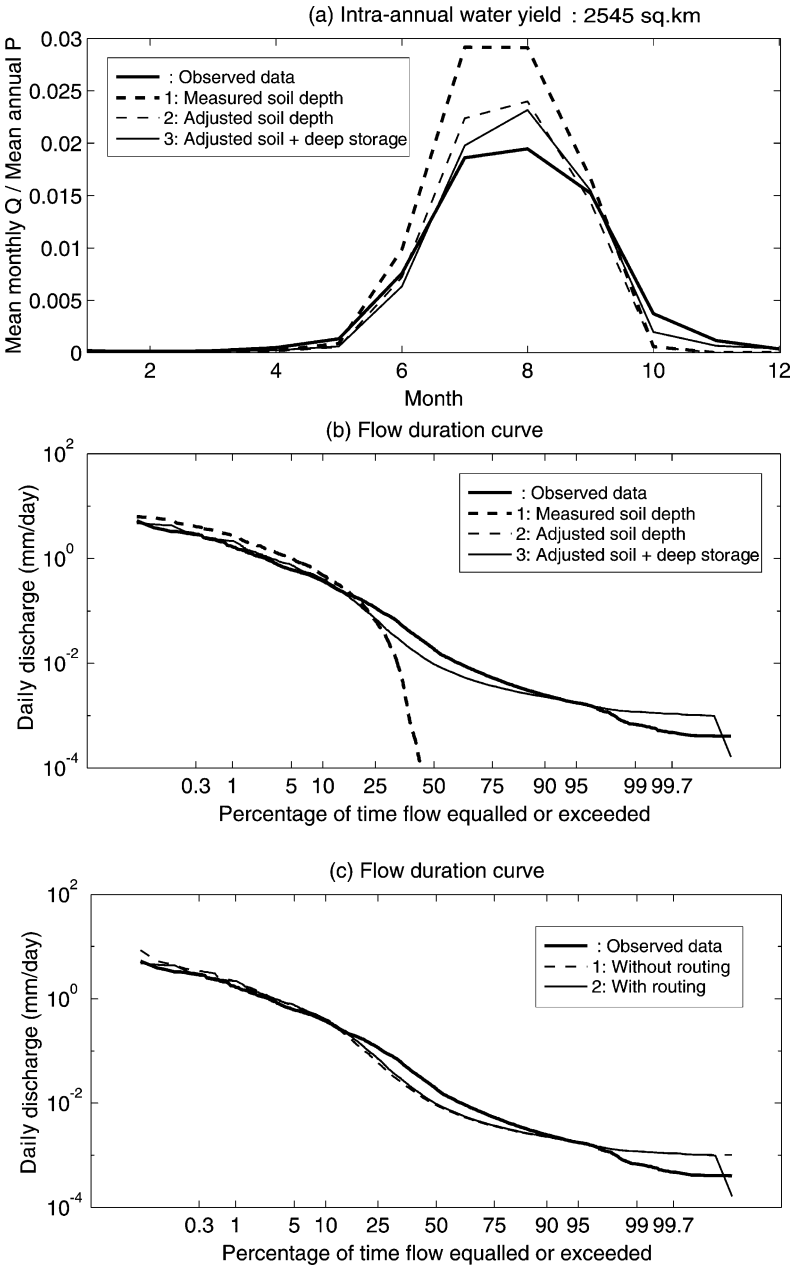

Fig. 12. Comparison of observed and simulated water yields between three simulation steps of the third-type model: (1) measured soil depth without deeper groundwater, (2) measured soil depths with deep groundwater store, and (3) adjusted soil depths with deep groundwater store, using the third type of models for the entire Collie catchment, 2545 km^2.(a) Intra-annual (mean monthly) water yield, (b) flow duration curve (based on daily flows), (c) comparison of the flow duration curves between two simulation steps: (1) without stream network routing and (2) with stream network routing.

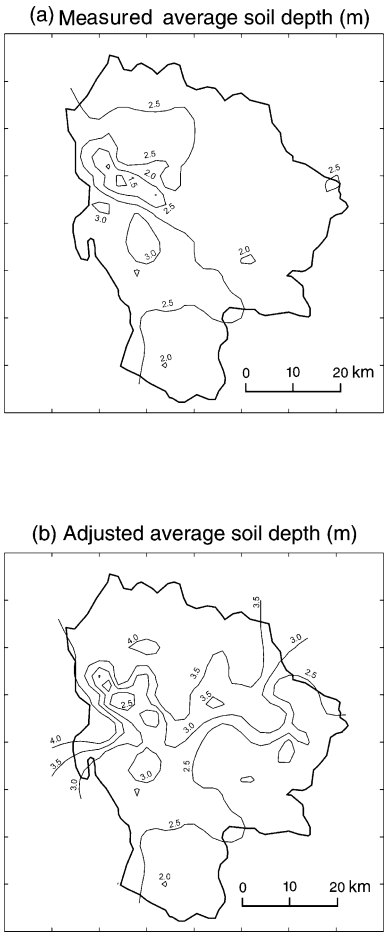

Fig. 13. Spatial pattern of average soil depths: (a) measured initial soil depths, and (b) adjusted soil depths.

in which we compare the intra-annual variation of runoff and the flow duration curve predicted by the model against those extracted from observed data. For the sake of brevity, we have selected three subcatchments for the presentation of detailed results: Cat-A (13 km^2), Cat-D (1344 km^2), and Cat-E (2545 km^2). Results for two other subcatchments, Cat-B (175 km^2) and Cat-C (633 km^2) are given in Jothityangkoon (2001). Table 3 presents the estimated parameter values for all subcatchments.

The results showed (those of Cat-A is presented here in Fig. 10) that it was possible to obtain very good fits for the smaller, upstream subcatchments, Cat-A (13 km^2), Cat-B (175 km^2) and Cat-C (633 km^2), although the deep groundwater component was slightly overestimated in Cat-B. This may be due to the constant ratio λ assumed for all subcatchments, or to the possibility that the deep groundwater contribution may not manifest itself until further downstream. This requires further careful field investigation, as the measured total runoff alone may not resolve this question.

On the other hand, in Cat-D (1344 km^2) and Cat-E (2545 km^2) the model using measured soil depths has tended to over-estimate the annual yields (not presented here) and the monthly variations are also over-predicted, as shown in Figs. 11(a) and 12(a). Flow duration curves are still poorly predicted. Sensitivity analyses carried out with the model parameters suggested that errors in the estimation of average soil depths may be responsible for these discrepancies. The soil depth distribution used in the model is based on soil profile data collected in the whole south-west region of Western Australia. Because of inadequate spatial coverage of the drilling conducted, the assumed values may not accurately represent the actual variability of soil depths within the Collie catchment.

The spatial pattern of average soil depths assumed in the model, shown in Fig. 13(a), suggests that it is almost uniform across the whole catchment, around the value of 2.5 m. Previous investigations of soil profiles and fluctuations of soil water content with depth in a number of experimental catchments in the eastern and northern parts of Collie showed that the change of water content in the soil profile was found to a depth about 6 m, suggesting deeper soils there (Sharma et al., 1987a). Thus, for the second simulation step, we experimented with the soil depths by increasing the average depth in the north and northeast of the catchment, without changing the shape of the distribution of soil depths used within the subcatchments. The spatial pattern of adjusted average soil depths is presented in Fig. 13(b).

The results of simulations using the adjusted soil depths are again shown in Figs. 11 and 12. They show that the slight adjustment of soil depths has led to improved results for intra-annual runoff variability in both Cat-D and Cat-E (inter-annual variabilities also improved but are not presented). Predictions of mean monthly runoff yield in the months of July and August are somewhat over-estimated, whereas predictions in October and November are still somewhat

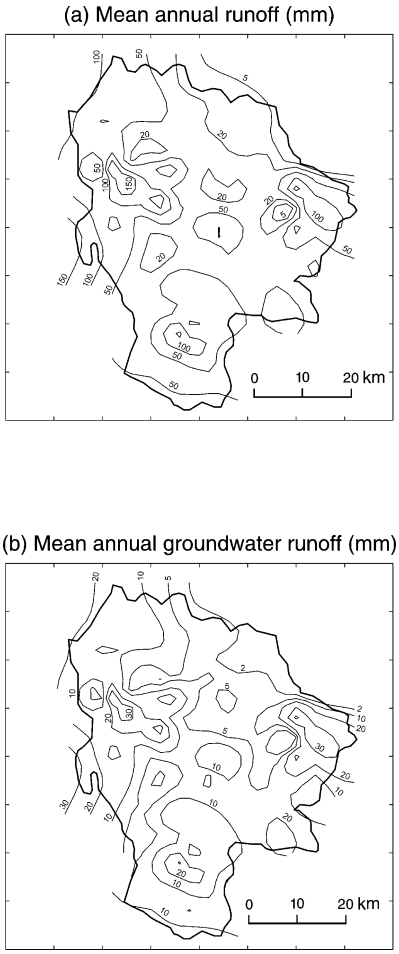

Fig. 14. Spatial pattern of estimated annual water balance based on adjusted soil depths: (a) mean annual water yield, and (b) mean annual yield from deep groundwater.

under-estimated [Figs. 11(a) and 12(a)]. Two possible reasons can be adduced for these discrepancies. One, the larger catchments may delay groundwater yield for many months through delays in the regional groundwater system. Secondly, there may still be considerable error in the soil depths that we have assumed. On the other hand, the addition of the deep groundwater store, in addition to the adjustment of soil depths, does significantly improve the flow duration curve [Figs. 11(b) and 12(b)], while the introduction of streamflow routing gives a better reproduction of high flows, but does not change low flows [Fig. 12(c)].

Fig. 14(a) presents the spatial pattern of mean annual water yield estimated by the final distributed water balance model (after adjustment of soil depths). Runoff is lowest in the north-west of the catchment where rainfall is low and the forest cover is high. The gradient of annual runoff yield is predominantly increasing in the east to west direction. A similar spatial pattern is shown for mean annual groundwater runoff [Fig. 14(b)]. The range is 2–30 mm going from east to west. The proportion of mean annual groundwater runoff estimated for the western parts of the catchment coincide well with estimates by Stokes (1985) and Johnston et al. (1983). No corresponding estimates are available for the eastern subcatchments. Note that these estimates of total runoff and its groundwater component are based on rather uncertain estimates of the soil depth distribution and the parameter λ, but are nevertheless useful indicators of spatial variability of water balance.

Finally, we present a comparison of the observed and simulated daily time series of runoff for two of the subcatchments considered before (Fig. 15). The comparisons point to two areas in which the model requires improvements, and they both relate to routing. The timing difficulties in the larger catchment suggests that the constant velocity parameter we use is not sufficient, and a variable velocity (dependent on discharge) will be useful. Secondly, the failure to capture the recessions in both catchments suggests that the use of constant a and b parameters for subsurface flow routing in hillslopes may not be sufficient. These are left for further research. Despite these discrepancies, it is clear that we have managed to obtain a good match to the observations, even though the parameters were estimated without any automatic calibration involving a comparison of these two time series. This suggests that the downward approach we have proposed based on the three signatures is a useful technique for the development of models for predictive purposes.

6. Discussion and conclusions

The paper has presented a systematic examination of the process controls on water balance at the annual, monthly and daily time scales. At each scale, we have endeavoured to develop parsimonious models, with the minimum complexity that is necessary to capture

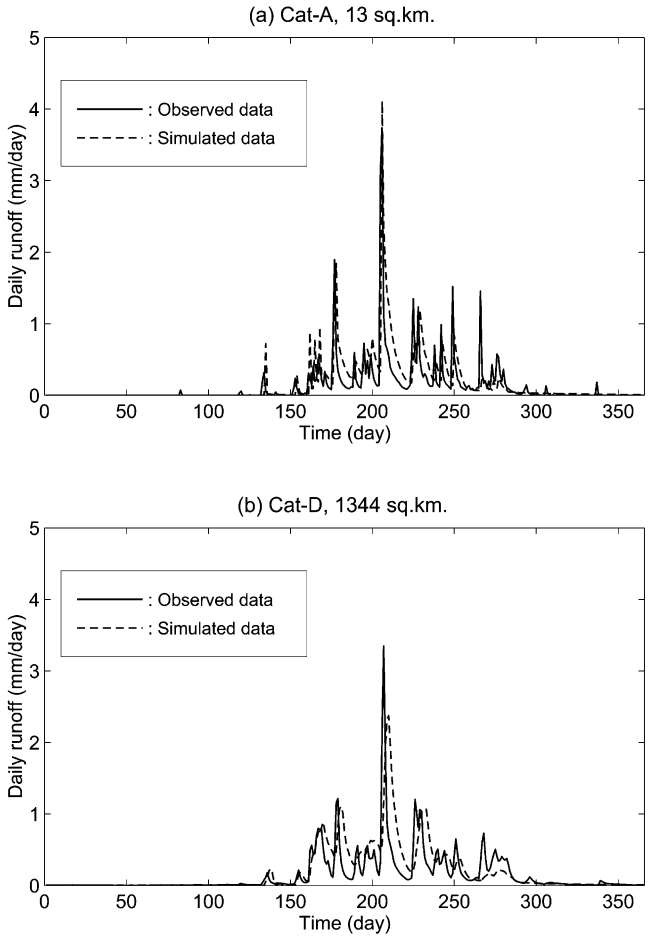

Fig. 15. Comparison of observed and simulated time series of daily runoff for two typical years, 1988. (a) Cat-A, 13 km^2, (b) Cat-D, 1344 km^2.

runoff variability, using the downward scaling approach of Klemes (1983). At each step, the simulation results are compared with observed data from the Collie River Basin in Western Australia through appropriate signatures of the runoff variability: inter-annual, intra-annual, and the flow duration curve (for daily runoff).

The first type of models we considered was based on annual climatic inputs, and consisted of a simple partitioning of annual rainfall into evaporation and saturation excess runoff. It was seen that this model could not reproduce the observed inter-annual variability of annual runoff yield, unless a number of different stores of varying sizes (ranging from small to large) are introduced to capture the spatial variability of soil depths. Indeed, it was found that, in this region, the spatial variability of soil depths was more important than subcatchment variability of annual rainfall. This model required only three parameters: soil depth, average porosity and a percentage interception loss.

The first type of models was found to be too simple to explain the intra-annual (mean monthly) variation of runoff yield. A second type of models was introduced which incorporated additional processes, especially the generation of subsurface runoff through a linear storage–discharge relationship, and a partitioning of evapotranspiration into bare soil evaporation and transpiration. These additional processes are modelled through additional parameters: four soil and topographic parameters and two vegetation

Table 4
Summary of process controls, and needed components and complexities for water balance modelling at the annual, monthly and daily scales

	Annual yield	Monthly yield	Daily yield
Model type	Fist type model	Second type model	Third type model
Time scale of input data	Annual data	Monthly data	Daily data
Storage–discharge relationship	Linear	Linear	Non-linear
Multiple buckets connection	Parallel	Parallel	Serial and parallel
Additional storage	–	–	Deep groundwater
Stream networks	–	–	Routing model
Parameters	D, ϕ, i	D, ϕ, i, f_c, L, $\tan\beta$, K_s, M, k_v	D, ϕ, i, f_c, a, b, λ, v, M, k_v

parameters. These additions were shown to produce good agreement between simulated results and observed data in terms of both the inter-annual and intra-annual runoff variabilities.

However, the second type of models was inadequate to reproduce the daily variation of runoff, especially at the subcatchment scale. Notably, the flow duration curves were not reproduced in the low flow range. In order to reproduce the three signatures of inter-annual, intra-annual variabilities, and the flow duration curve, a third type of models was developed. It introduced (1) a non-linear storage–discharge relationship for the subsurface runoff generation process, (2) multiple stores in series based on the empirical distribution of soil depths, and most crucially, (3) a deeper groundwater store. Stream network routing was introduced for a distributed model of the large catchment response. The total number of parameters for the third type of models is ten: seven soil and topographic parameters, two vegetation parameters, and one routing parameter, all of which were estimated without calibration. Of these ten parameters, only two, namely the subsurface drainage parameters a and b, were estimated from analysis of recession curves, and not from landscape features. In other words, while they were estimated outside of the rainfall-runoff models presented, they nevertheless require the availability and analysis of observed streamflows. Future work should endeavour to find ways to estimate these parameters directly from landscape features to enable predictions of ungauged catchments.

The processes and complexities necessary for the prediction of annual, monthly and daily runoff variabilities are summarized in Table 4. At all time scales spatial variability of soil depths was demonstrated to be the most dominant factor governing runoff variability in this region, followed by spatial variability of climate and vegetation. This suggests that significant improvements can be made to modelling capability if more precise information on the distribution of soil depths can be generated based on prior field studies.

In this paper, and in all companion papers using the downward approach, we have only used the signature plots as the basis of systematically increasing model complexity. The model performances could of course be studied by means of traditional measures such as the Nash and Sutcliffe efficiency. However, we feel that the focus on signature plots, as opposed statistical performance measures, would help direct our research efforts towards physical interpretation of catchment functioning, as opposed to model improvements and calibration. In other words, mere curve fitting that the Nash and Sutcliffe efficiency focuses on does not provide physical insights, which is what is needed for prediction of ungauged catchments.

The systematic, downward modelling approach presented in this paper, and in other companion papers (Farmer et al., 2001; Atkinson et al., 2001; Eder et al., 2001) should be repeated in other climatic regions. They can, in the long-term, give rise to deeper understanding of the climate, soil and vegetation controls on water balance across large regions, and can lead to more parsimonious models in the future.

Acknowledgements

This work was financially supported by the Royal Thai Government scholarship awarded to the first author. The work was also partially supported by an

ARC Small Grant awarded to the second author through the University of Western Australia. We thank the two reviewers G. Blöschl and D. Post for their constructive comments which helped to substantially improve the paper. CWR Reference ED 1553 CJ.

References

Abbott, M.B., Bathurst, J.C., Cunge, J.A., O'Connell, P.E., Rasmussen, J., 1986. SHE—1: history and philosophy of a physically-based, distributed modelling system. J. Hydrol. 87, 45–59.

Atkinson, S.E., Sivapalan, M., Woods, R.A., 2001. Climate, soil, vegetation controls on water balance model complexity over changing time scales. Water Resour. Res. (in preparation).

Bathurst, J.C., 1992. Future of distributed modelling: Systeme Hydrologique Europeen. J. Hydrol. 6, 265–277.

Bettenay, E., Russell, W.G.R., Hudson, D.R., Gilkes, R.J., Edmiston, R.J., A description of experimental catchment in the Collie area, Western Australia. CSIRO Aust. Div. Land Resour. Manage., Tech. Pap. No. 7, 1980.

Beven, K.J., 1989. Changing ideas in hydrology: the case of physically-based models. J. Hydrol. 105, 157–172.

Blöschl, G., Sivapalan, M., 1995. Scale issues in hydrological modelling: a review. Hydrol. Process. 9 (3/4), 251–290.

Boughton, W.C., 1984. A simple model for estimating the water yield of ungauged catchments. Civ. Eng. Trans. Inst. Aust. CE (26), 83–88.

Department of Conservation and Environment, 1980. Atlas of Natural Resources, Darling System, Western Australia. University of Western Australia Press, Perth, Western Australia.

Eagleson, P.S., 1978. Climate soil, and vegetation 1: introduction to water balance dynamics. Water Resour. Res. 14 (5), 705–712.

Eder, G., Sivapalan, M., Nachtnebel, H.P., 2001. Modeling water balances in Alpine catchment through exploitation of emergent properties over changing time scales. Hydrol. Process (submitted for publication).

Farmer, D.F., Sivapalan, M., Jothityangkoon, C., 2001. Climate, soil and vegetation controls upon the variability of water balance in temperate and semi-arid landscapes: downward approach to hydrological prediction. Water Resour. Res. (submitted for publication).

Freeze, R.A., 1978. Mathematical models of hillslope hydrology. In: Kirkby, M.J. (Ed.). Hillslope Hydrology. John Wiley & Sons, Chichester, UK, pp. 177–225 Chapter 6.

Gupta, V.K., Waymire, E., 1998. Spatial variability and scale invariance in hydrological regionalization. In: Sposito, G. (Ed.). Scale Invariance and Scale Dependence in Hydrology. Cambridge University Press, Cambridge, UK, pp. 88–135.

Jakeman, A.J., Hornberger, G.M., 1993. How much complexity is warranted in a rainfall-runoff model?. Water Resour. Res. 29, 2637–2649.

Johnston, C.D., Hurle, D.H., Hudson, D.R., Height, M.I., 1983. Water movement through preferred paths in lateritic profiles of the Darling Plateau, Western Australia. Tech. paper no. 1, CSIRO Division Groundwater Research, Perth.

Jothityangkoon, C., 2001. Space–time variability and scaling of hydrologic response and role of catchment water balance. Unpublished PhD dissertation. Ctre. for Water Res., Univ. of West. Aust., Crawley.

Klemes, V., 1983. Conceptualisation and scale in hydrology. J. Hydrol. 65, 1–23.

Manabe, S., 1969. Climate and ocean circulation—1: the atmospheric circulation and the hydrology of the earth's surface. Monthly Weather Review 97 (11), 739–774.

Milly, P.C.D., 1994. Climate, soil water storage, and the average annual water balance. Water Resour. Res. 30 (7), 2143–2156.

O'Connell, P.E., Todini, E., 1996. Modelling of rainfall, flow and mass transport in hydrological systems: an overview. J. Hydrol. 175, 3–16.

Reggiani, P., Sivapalan, M., Hassanizadeh, S.M., 1998. A unifying framework for watershed thermodynamics: balance equations for mass, momentum, energy, entropy and the 2nd law of thermodynamics. Adv. in Water Resour. 22 (4), 367–398.

Reggiani, P., Hassanizadeh, S.M., Sivapalan, M., Gray, W.G., 1999. A unifying framework for watershed thermodynamics: constitutive relationships. Adv. in Water Resour. 23 (1), 15–39.

Reggiani, P., Sivapalan, M., Hassanizadeh, S.M., 2000. Conservation equations governing hillslope responses: exploring the physical basis of water balance. Water Resour. Res. 36 (7), 1845–1864.

Reggiani, P., Sivapalan, M., Hassanizadeh, S.M., Gray, W.G., 2001. Coupled equations for mass and momentum balance in a stream network: theoretical derivation and computational experiments. Proc. Royal Soc. (London), Ser. A 457, 157–189.

Sharma, M.L., Barron, R.J.W., Williamson, D.R., 1987a. Soil water dynamics of lateritic catchments as affected by forest clearing for pasture. In: Peck A.J., Williamson, D.R., (Eds.), Hydrology and Salinity in the Collie River Basin, Western Australia. J. Hydrol. 94, 29–46.

Sharma, M.L., Barron, R.J.W., Fernie, M.S., 1987b. Areal distribution of infiltration parameters and some soil physical properties in lateritic catchments. In Peck, A.J., Williamson, D.R., (Eds.), Hydrology and Salinity in the Collie River Basin, Western Australia. J. Hydrol. 94, 109–127.

Sivapalan, M., Ruprecht, J.K., Viney, N.R., 1996a. Water and salt balance modelling to predict the effect of land use changed in forested catchments—1: small catchment water balance model. Hydrol. Process. 10, 393–411.

Sivapalan, M., Viney, N.R., Ruprecht, J.K., 1996b. Water and salt balance modelling to predict the effect of land use changed in forested catchments—3: the large catchment model. Hydrol. Process. 10, 429–446.

Sivapalan, M., Woods, R.A., 1995. Evaluation of the effects of general circulation models' subgrid variability and patchiness of rainfall and soil moisture on land surface water balance fluxes. Hydrol. Process. 9, 453–473.

Stokes, R.A., 1985. Stream water and chloride generation in a small forested catchment in south western Australia. Masters Thesis, Dep. Civ. Eng., Univ. West. Aust.

Viney, N.R., Sivapalan, M., 1995. LASCAM: The large scale

catchment model. User manual, Report number WP 1070 NV, Ctre. For Water Res., Univ. West. Aust., 199 pp.

Williamson, D.R., Stokes, R.A., Ruprecht, J.K., 1987. Response of input and output of water and chloride to clearing for agriculture. In: Peck, A.J., Williamson, D.R. (Eds.), Hydrology and Salinity in the Collie River Basin, Western Australia. J. Hydrol. 94, 1–28.

Wittenberg, H., 1994. Nonlinear analysis of flow recession curves. IAHS Publ. 221, 61–67.

Wittenberg, H., 1999. Baseflow recession and recharge as a nonlinear storage processes. Hydrol. Process. 13, 715–726.

Wittenberg, H., Sivapalan, M., 1999. Watershed groundwater balance estimation using streamflow recession analysis and baseflow. J. Hydrol. 219, 20–33.

Ye, W., Bates, B.C., Viney, N.R., Sivapalan, M., 1997. Performance of conceptual rainfall-runoff models in low-yielding ephemeral catchments. Water Resour. Res. 33 (1), 153–166.